CCECE 2014 1569880189

DRDC-RDDC-2014-P101

Hybrid Localization of an Emitter by Combining Angle-of-Arrival and Received Signal Strength Measurements

Y.T. Chan[1], F. Chan[1], W. Read[2], B.R. Jackson[2], B.H. Lee[1]

[1]Dept. of Electrical and Computer Engr., Royal Military College of Canada, Kingston, Ontario
[2]Defence Research and Development Canada, Ottawa, Ontario

***Abstract*— Emitter localization, using different types of sensors and integrating their output properly can potentially increase localization accuracy. It is relatively easy to measure the received signal strength (RSS), but RSS localization is generally less accurate than angle-of-arrival (AOA) localization in most practical environments. When both RSS and AOA are available, fusing their measurements can improve localization accuracy. This paper develops a set of linear equations that optimally combines both AOA and RSS measurements, and is suitable for solution by weighted least squares. The simulation results show that at sufficiently low noise, the hybrid scheme is near optimal.**

Keywords—localization; angle-of-arrival; received signal strength; weighted least squares; Cramer Rao lower bound

1. INTRODUCTION

Passive localization of an emitter from its radio frequency (RF) transmissions has many applications such as search and rescue, electronic surveillance, cognitive radio networks, and wireless sensors networks [1-5]. A localization system consists of receivers (sensors) at known coordinates measuring signal characteristics from an emitter. Most commonly, the sensors measure the incoming signal's angle-of-arrival (AOA), time-of-arrival (TOA), time-difference-of-arrival (TDOA), or received signal strength (RSS). These parameters generate emitter position loci, whose intersection gives the emitter position. For AOA, the loci are bearing lines originating from the sensors. For TDOA, they are hyperbolae with the foci at the sensors. For RSS and TOA, they are circles centered at the sensors. The reverse holds in the case of self-localization. For example in navigation, a receiver uses the signals from multiple emitters (GPS satellites) at known positions to determine its own position.

Due to measurement noises, the loci do not intersect at a single point. Thus, it is necessary to devise algorithms to minimize the effects of noise and give a single solution for the emitter position. There are broadly two types of algorithms [6]: maximum likelihood (ML) and linear least squares (LLS). The main advantage of ML is that it is optimum, i.e., the position estimate has minimal mean squared errors. However, ML requires iteration, and has no guarantee of convergence to the global minimum because of a multi-nodal cost function. In contrast, LLS [7] is closed-form, easy to compute, but is only optimal when the noise power is sufficiently small. The majority of estimators use LLS.

Recently, there has been research on the use of unmanned aerial vehicles (UAV) for localization, due to advances in UAV sensor technology and their increasing capability and availability [8-11]. Localization with a UAV is a three dimensional (3-D) problem and extending 2D algorithms to 3D is not straight-forward in all cases. Since RSS is easy to obtain, as compared to TDOA which requires precise and relatively expensive equipment, it has become popular for lower cost wireless sensor network applications [3]. However, RSS localization generally has lower accuracy than TDOA or AOA. This is because it is difficult to accurately model signal propagation in a practical measurement environment and the fading effects in particular are difficult to quantify. This paper proposes augmenting RSS with AOA for 3D localization which could be available from UAV or aircraft. While very simple RF receivers can measure RSS with a single antenna, to measure azimuth and elevation AOA of an incoming signal, antenna arrays can be used or a UAV can use rotational and tilting antennas [10].

Some recent work on hybrid localization [12-14] is in 2D. In [12], the hybrid components are RSS and AOA, but optimal weights were not used. Instead, [12] studied the localization performance as a function of the relative weighting between RSS and AOA. Combining RSS, TOA and TDOA, [13] compared the performance of weighted least squares (WLS) against ML. However, because the WLS equations are sub-optimal, its performance is below ML. The hybrid in [14] consists of RSS, TOA, TDOA, and AOA. It applies a Taylor series approximation to linearize the equations. This necessitates iterations as updates to the equilibrium emitter position will continue until convergence.

In the following, Section 2 develops a hybrid localization scheme that combines RSS with AOA. Both RSS and AOA are nonlinear functions of the unknown emitter coordinates. However, the nonlinear equations become linear when the nonlinear terms are taken as an additional unknown. A standard weighted least squares gives a first solution, assuming all unknowns are independent. Section 3 links the variables through a known constraint to improve accuracy. The simulation results are presented in Section 4. As expected,

978-1-4799-3010-9/14/$31.00 ©2014 IEEE

hybrid performance improves the performance over AOA and RSS alone. However, if the AOA (or RSS) measurements have a much higher accuracy than the other, then hybrid is just as good as AOA (or RSS). The conclusions are presented in Section 5.

2. HYBRID 3D LOCALIZATION

This section begins with the development of the RSS localization equations, followed by AOA, and then the combination of both.

2.1. RSS Localization

Let there be N sensors at known locations (x_i, y_i, z_i), $i = 1,\ldots,N$. The emitter is at unknown location (x, y, z). Each sensor receives from the emitter [3]

$$P_i = \eta_0 R_i^{-\alpha} 10^{\frac{n_i}{10}}, \tag{1}$$

where P_i is the RSS at the i-th sensor, η_0 is the unknown emitter reference power, α is the known path loss exponent, $2 \le \alpha \le 6$, and n_i is a zero-mean Gaussian random variable (zmgrv) of known variance σ_s^2. Normally P_i is the average of several measurements so that the measurement noise is negligible compared to shadow-fading effects which n_i represents. The unknown distance to an emitter is given by:

$$R_i = \left[(x-x_i)^2 + (y-y_i)^2 + (z-z_i)^2\right]^{\frac{1}{2}}. \tag{2}$$

Eliminating the unknown η_0 by taking ratios of P_i yields

$$r_{1i}^{2/\alpha} = \left(\frac{P_1}{P_i}\right)^{2/\alpha} = \frac{R_i^2}{R_1^2} e^{\beta(n_i - n_1)} \tag{3}$$

where

$$\beta = -2\ln 10/(10\alpha). \tag{4}$$

In (3), sensor 1 (R_1, P_1) is the reference for the ratios. Its selection is arbitrary and does not cause a loss of generality. Any other R_i as a reference will not affect the estimation results [15].

Let the unknown vector be

$$\mathbf{q} = \left[\frac{x-x_1}{R_1^2} \quad \frac{y-y_1}{R_1^2} \quad \frac{z-z_1}{R_1^2} \quad \frac{1}{R_1^2}\right]^T. \tag{5}$$

For sufficiently small $(n_i - n_1)$ in (3),

$$e^{\beta(n_i - n_1)} \approx 1 + \beta(n_i - n_1). \tag{6}$$

Also, let

$$\begin{aligned} &x_{1i} = x_1 - x_i, \quad y_{1i} = y_1 - y_i, \\ &z_{1i} = z_1 - z_i, \quad k_{1i} = x_{1i}^2 + y_{1i}^2 + z_{1i}^2. \end{aligned} \tag{7}$$

Stacking the $i = 2,\ldots,N$ equations from (3) yields the RSS matrix equation

$$\mathbf{A}_s \mathbf{q} \approx \mathbf{v}_s + \boldsymbol{\gamma}_s \tag{8}$$

where

$$\mathbf{A}_s = \begin{bmatrix} 2x_{12} & 2y_{12} & 2z_{12} & k_{12} \\ \vdots & \vdots & \vdots & \vdots \\ 2x_{1N} & 2y_{1N} & 2z_{1N} & k_{1N} \end{bmatrix}_{(N-1)\times 4} \tag{9}$$

is the system matrix,

$$\mathbf{v}_s = \left[r_{12}^{2/\alpha} - 1 \quad \cdots \quad r_{1N}^{2/\alpha} - 1\right]^T_{(N-1)\times 1} \tag{10}$$

is the measurement vector, and

$$\boldsymbol{\gamma}_s = \left[\frac{R_2^2}{R_1^2}(n_2 - n_1) \quad \cdots \quad \frac{R_N^2}{R_1^2}(n_N - n_1)\right]^T_{(N-1)\times 1} \tag{11}$$

is the shadow fading vector.

2.2. AOA Localization

In addition to RSS, the N sensors also measure the signal's incoming azimuth angle,

$$\theta_i = \bar{\theta}_i + \varepsilon_i \tag{12}$$

and elevation

$$\varphi_i = \bar{\varphi}_i + e_i, \tag{13}$$

where $\bar{\theta}_i$ and $\bar{\varphi}_i$ are respectively the true azimuth and elevation angles with respect to the i-th sensor. The measurement noise components are represented by ε_i and e_i. They are independent zmgrv with variances σ_θ^2 and σ_φ^2, respectively.

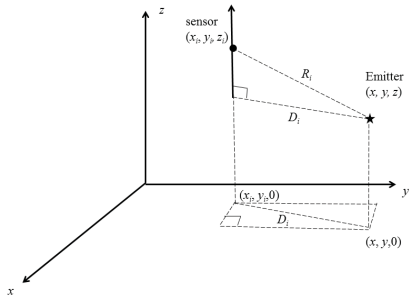

Figure 1: Angle and distance convention.

The distance and AOA conventions are shown in Figure 1, where

$$D_i \sin\bar{\theta}_i = x - x_i \tag{14}$$

and

$$D_i \cos\bar{\theta}_i = y - y_i \tag{15}$$

so that

$$D_i^2 = (x-x_i)^2 + (y-y_i)^2. \tag{16}$$

Also

$$R_i \sin\bar{\varphi}_i = D_i \tag{17}$$

and

$$R_i \cos\bar{\varphi}_i = z - z_i. \tag{18}$$

Substituting (12) into (14) and (15) and expanding the sum of sin and cos result in

$$x - x_i \approx D_i \sin\theta_i - \varepsilon_i D_i \cos\theta_i \tag{19}$$

and

$$y - y_i \approx D_i \cos\theta_i + \varepsilon_i D_i \sin\theta_i. \tag{20}$$

The approximation in (19) and (20) come from $\cos\varepsilon_i \approx 1$ and $\sin\varepsilon_i \approx \varepsilon_i$, which is valid for sufficiently small ε_i.

Multiplying (19) by $\cos\theta_i$ and (20) by $\sin\theta_i$ and subtracting the equations give:

$$(y-y_i)\sin\theta_i-(x-x_i)\cos\theta_i \approx \varepsilon_i D_i \tag{21}$$

Multiplying (19) by $\sin\theta_i$ and (20) by $\cos\theta_i$ and adding give:

$$(x-x_i)\sin\theta_i+(y-y_i)\cos\theta_i \approx D_i \tag{22}$$

Repeating the same procedure as above with (13), (17) and (18) produces

$$R_i\sin\varphi_i - e_i R_i\cos\varphi_i \approx D_i \tag{23}$$

and

$$R_i\cos\varphi_i + e_i R_i\sin\varphi_i \approx z-z_i. \tag{24}$$

Let (22) replace D_i in (23). Multiplying (23) by $\cos\varphi_i$, (24) by $\sin\varphi_i$ and subtracting yields

$$(z-z_i)\sin\varphi_i-[(x-x_i)\sin\theta_i+(y-y_i)\cos\theta_i]\cos\varphi_i \approx e_i R_i. \tag{25}$$

Dividing (25) by R_i^2 and stacking the i=1,…,N equations give the AOA matrix equation

$$\mathbf{A}_A\mathbf{q} \approx \mathbf{v}_A + \boldsymbol{\gamma}_A \tag{26}$$

where the system matrix

$$\mathbf{A}_A = \begin{bmatrix}\mathbf{A}_1 & \mathbf{A}_2\\ \mathbf{A}_3 & \mathbf{A}_4\end{bmatrix}_{2N\times 4} \tag{27}$$

with

$$\mathbf{A}_1 = \begin{bmatrix}-a_1 & b_1 & 0\\ \vdots & \vdots & \vdots\\ -a_N & b_N & 0\end{bmatrix}_{N\times 3} \quad \mathbf{A}_2 = \begin{bmatrix}0\\ x_{12}a_2+y_{12}b_2\\ \vdots\\ x_{1N}a_N+y_{1N}b_N\end{bmatrix}_{N\times 1}$$

$$\mathbf{A}_3 = \begin{bmatrix}-b_1c_1 & -a_1c_1 & d_1\\ \vdots & \vdots & \vdots\\ -b_Nc_N & -b_Nc_N & d_N\end{bmatrix}_{N\times 3}$$

$$\mathbf{A}_4 = \begin{bmatrix}0\\ -x_{12}b_2d_2-y_{12}a_2d_2+z_{12}b_2\\ \vdots\\ -x_{1N}b_Nd_N-y_{1N}a_Nd_N+z_{1N}b_N\end{bmatrix}_{N\times 1} \tag{28}$$

and $a_i = \cos\theta_i$, $b_i = \sin\theta_i$, $c_i = \cos\varphi_i$, $d_i = \sin\varphi_i$.

The measurement vector is

$$\mathbf{v}_A = [0 \;\cdots\; 0 \,|\, 0 \;\cdots\; 0]^T_{2N\times 1}, \tag{29}$$

and the noise vector is given by

$$\boldsymbol{\gamma}_s = \left[\frac{D_1\varepsilon_1}{R_1^2} \;\cdots\; \frac{D_N\varepsilon_N}{R_1^2} \,\middle|\, \frac{R_1e_1}{R_1^2} \;\cdots\; \frac{R_Ne_N}{R_1^2}\right]^T_{2N\times 1}. \tag{30}$$

Note that (26) is different from (16) in [16]. The increase in dimension of the unknown vector to 4x1 is necessary here to ensure that both AOA and RSS have the same unknown vector.

2.3. Hybrid Localization

Combining (8) and (26) give the hybrid equation

$$\mathbf{A}\mathbf{q} \approx \mathbf{v}+\boldsymbol{\gamma} \tag{31}$$

where

$$\mathbf{A} = \begin{bmatrix}\mathbf{A}_A\\ \mathbf{A}_s\end{bmatrix}, \quad \mathbf{v} = \begin{bmatrix}\mathbf{v}_A\\ \mathbf{v}_s\end{bmatrix}, \qquad \boldsymbol{\gamma} = \begin{bmatrix}\boldsymbol{\gamma}_A\\ \boldsymbol{\gamma}_s\end{bmatrix} \tag{32}$$

The weighted least squares (WLS) estimate for (31) is

$$\hat{\mathbf{q}} = (\mathbf{A}^T\mathbf{W}\mathbf{A})^{-1}\mathbf{A}^T\mathbf{W}\mathbf{v}, \tag{33}$$

and the inverse of the weight matrix is given by:

$$\mathbf{W}^{-1} = E\{\boldsymbol{\gamma}\boldsymbol{\gamma}^T\} = \begin{bmatrix}\sigma_\theta^2\begin{bmatrix}D_1^2 & 0 & 0\\ 0 & \ddots & 0\\ 0 & 0 & D_N^2\end{bmatrix} & & \\ & \sigma_\varphi^2\begin{bmatrix}R_1^2 & 0 & 0\\ 0 & \ddots & 0\\ 0 & 0 & R_N^2\end{bmatrix} & \\ & & \frac{1}{R_1^4}\sigma_s^2\beta^2\begin{bmatrix}2R_2^4 & R_2^2R_3^2 & \cdots & R_2^2R_N^2\\ R_3^2R_2^2 & 2R_3^4 & \cdots & \vdots\\ & & \ddots & \\ & & & 2R_N^4\end{bmatrix}\end{bmatrix} \tag{34}$$

Some remarks on the WLS of (33):

1. In (34), the D_i and R_i are unknowns. Initially (33) uses $R_i^2 = P_i^{-2/\alpha}$ and $D_i^2 = R_i^2\sin^2\varphi_i$. It then updates these values by the estimates of $\hat{\mathbf{q}}$. Only a single update is necessary.
2. There is a dependency among the elements in $\mathbf{q}$. Let
$$\mathbf{q} = [q_1 \quad q_2 \quad q_3 \quad q_4]^T. \tag{35}$$
It then follows from (5) that
$$q_1^2+q_2^2+q_3^2 = q_4. \tag{36}$$

The WLS in (33) ignores this dependency. A second WLS (SWLS) that forces (36) onto the q_i will provide more accurate estimates. The development of SWLS is in the next Section .

3. The Second Weighted Least Squares

Substituting (31) into (33) gives

$$\hat{\mathbf{q}} = (\mathbf{A}^T\mathbf{W}\mathbf{A})^{-1}\mathbf{A}^T\mathbf{W}(\mathbf{A}\mathbf{q}-\boldsymbol{\gamma}). \tag{37}$$

Since $\boldsymbol{\gamma}$ contains a zmgrv,

$$E\{\hat{\mathbf{q}}\} = \mathbf{q} \tag{38}$$

then (33) is unbiased. Let

$$\boldsymbol{\chi} = \hat{\mathbf{q}}-\mathbf{q} = [w_1 \quad w_2 \quad w_3 \quad w_4]. \tag{39}$$

The covariance of $\hat{\mathbf{q}}$ is

$$\begin{aligned}E\{\boldsymbol{\chi}\boldsymbol{\chi}^T\} &= \mathrm{cov}\{\hat{\mathbf{q}}\}\\ &\approx (\mathbf{A}^T\mathbf{W}\mathbf{A})^{-1}\mathbf{A}^T\mathbf{W}E\{\boldsymbol{\gamma}\boldsymbol{\gamma}^T\}\mathbf{W}\mathbf{A}(\mathbf{A}^T\mathbf{W}\mathbf{A})^{-1}\\ &\approx (\mathbf{A}^T\mathbf{W}\mathbf{A})^{-1}.\end{aligned} \tag{40}$$

Applying (36) to the $\hat{q}_i$ gives

$$\underbrace{\begin{bmatrix}1&0&0\\0&1&0\\0&0&1\\1&1&1\end{bmatrix}}_{\mathbf{G}}\begin{bmatrix}q_1^2\\q_2^2\\q_3^2\end{bmatrix}=\underbrace{\begin{bmatrix}\hat{q}_1^2\\\hat{q}_2^2\\\hat{q}_3^2\\\hat{q}_4\end{bmatrix}}_{\mathbf{h}}+\underbrace{\begin{bmatrix}\xi_1\\\xi_2\\\xi_3\\\xi_4\end{bmatrix}}_{\boldsymbol{\xi}}, \tag{41}$$

where $\boldsymbol{\xi}$ is the error vector, whose elements are

$$\begin{aligned}\xi_1 &= q_1^2-\hat{q}_1^2 = q_1^2-(q_1+w_1)^2 \approx -2q_1w_1,\\ \xi_2 &\approx -2q_2w_2,\\ \xi_3 &\approx -2q_3w_3,\\ \xi_4 &\approx w_4.\end{aligned} \tag{42}$$

The SWLS of (41) is

$$\begin{bmatrix}\tilde{q}_1^2\\\tilde{q}_2^2\\\tilde{q}_3^2\end{bmatrix}=(\mathbf{G}^T\boldsymbol{\Psi}^{-1}\mathbf{G})^{-1}\mathbf{G}^T\boldsymbol{\Psi}^{-1}\mathbf{h}. \tag{43}$$

The inverse of the weight matrix is

$$\boldsymbol{\Psi}^{-1}=E\{\boldsymbol{\xi}\boldsymbol{\xi}^T\}=\mathbf{F}\,\mathrm{cov}(\hat{\mathbf{q}})\mathbf{F} \tag{44}$$

where

$$\mathbf{F}=\mathrm{diag}\begin{bmatrix}-2q_1 & -2q_2 & -2q_3 & 1\end{bmatrix} \tag{45}$$

The estimate of the emitter position is

$$\begin{bmatrix}\hat{x}\\\hat{y}\\\hat{z}\end{bmatrix}=\begin{bmatrix}\dfrac{\pm\sqrt{\tilde{q}_1^2}}{\hat{q}_4}+x_1\\[2ex]\dfrac{\pm\sqrt{\tilde{q}_2^2}}{\hat{q}_4}+y_1\\[2ex]\dfrac{\pm\sqrt{\tilde{q}_3^2}}{\hat{q}_4}+z_1\end{bmatrix}. \tag{46}$$

When the noise power is high, a $\tilde{q}_i^2$ could become negative. Then SWLS has no solution and WLS of (33) is the answer. If all $\tilde{q}_i^2$ are positive, then there are eight possible combinations in (46). Each gives a different J defined in the Appendix (53). The estimate is the combination that gives the smallest J.

4. Simulation Results

The simulation experiments aim to corroborate the theoretical developments in Sections 2 and 3, and to evaluate the accuracy improvement due to hybrid localization, over the individual AOA or RSS localization.

The localization geometry has N=6 sensors at (0, 1, 0.3), (0.5, 0.5, 0.3), (1, 0, 0.3), (-0.5, 0.5, 0.3), (1, 0.3, 0.3), (1, -1, 0.3), and the emitter is either 'inside' or 'outside' the perimeter of the sensors. For RSS, $\alpha = 3$ and $\eta_0 = 1$ in (1). For 500 independent trials, the Root Mean Square Error is

$$\mathrm{RMSE}=\left\{\frac{\sum_{k=1}^{500}\left[(\hat{x}(k)-x)^2+(\hat{y}(k)-y)^2+(\hat{z}(k)-z)^2\right]}{500}\right\}^{\frac{1}{2}} \tag{47}$$

where $(\hat{x}(k),\hat{y}(k),\hat{z}(k))$ is the k-th estimate.

For the 'inside' case, the emitter is at (0, 0.5, 0). Figure 2 plots the RMSE as σ_s varies from 0.01 to 1, at a constant σ_θ=σ_φ=1°. The figure also contains the Root Cramer Rao Lower Bound (RCRLB) (see Appendix) for hybrid, AOA and RSS localizations.

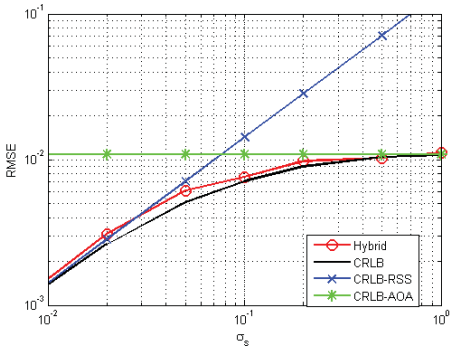

Figure 2: Simulation results for the 'inside' case, variable σ_s, fixed σ_θ= σ_φ= 1°.

There are several things to note in this figure:

1. The hybrid RMSE coincides with the RCRLB, confirming that the SWLS is near optimal for sufficiently small noise.
2. For σ_s below 0.02, RSS alone has a much higher accuracy than AOA alone. Hence hybrid RMSE ≈ RSS-RCRLB. The opposite occurs when σ_s>0.5.
3. The benefits of hybrid localization occur in the range of 0.02 ≤σ_s ≤0.5, when the hybrid RMSE is below the individual RCRLB of both the AOA and RSS.

Figure 3 shows a similar pattern but with σ_s fixed at 0.8 and σ_θ=σ_φ varied from 0.2 to 5 degrees.

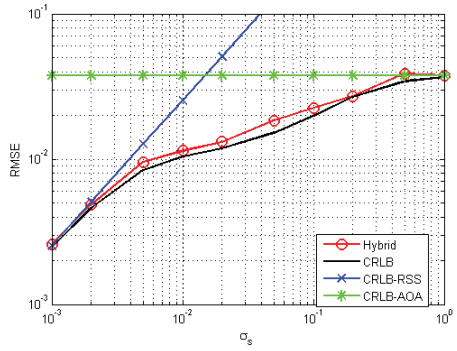

Figure 3: Simulation results for the 'outside' case, variable σ_s, fixed σ_θ= σ_φ= 1°.

Figures 4 and 5 are similar to Figures 2 and 3, except the emitter is 'outside' at (0.2, 1.9, 0). The 'outside' case generally has a less favorable localization geometry than 'inside'. The RCRLB in lower than those in Figures 4 and 5.

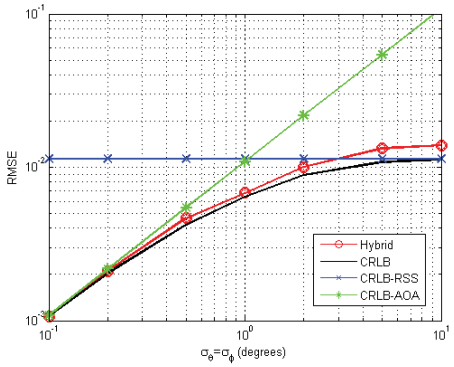

Figure 4: Simulation results for the 'inside' case, variable $\sigma_\theta = \sigma_\varphi$, fixed $\sigma_s = 0.8$.

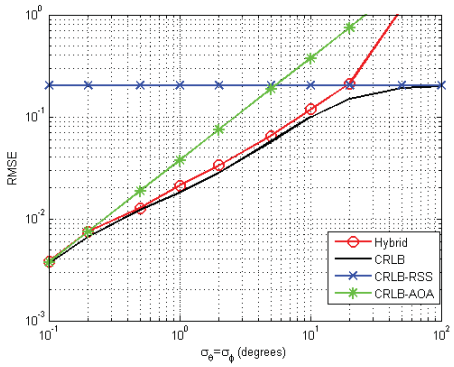

Figure 5: Simulation results for the 'outside' case, variable $\sigma_\theta = \sigma_\varphi$, fixed $\sigma_s = 0.8$.

5. CONCLUSIONS

This paper has formulated a set of linear equations for hybrid localization by fusing AOA and RSS measurements. This enables a closed-form solution, first by WLS and then by a second WLS. Simulation results are close to the Cramer Rao Lower Bound. The hybrid technique is able to improve localization accuracy over using AOA or RSS alone.

APPENDIX

For RSS only, the ML function is

$$J_s = \frac{1}{2\sigma_s^2}\left[(N-1)\sum_{i=2}^{N}\bar{g}_i^2 - \sum_{i=2}^{N}\sum_{\substack{j=2 \\ i\neq j}}^{N}\bar{g}_i\bar{g}_j\right] \quad (49)$$

where

$$\bar{g}_i = \ln r_{1i}^{2/\alpha} - \ln\frac{\hat{R}_i^2}{\hat{R}_1^2},$$

$$\hat{R}_i^2 = (\hat{x}-x_i)^2 + (\hat{y}-y_i)^2 + (\hat{z}-z_i)^2. \quad (50)$$

For AOA only, the ML function is

$$J_A = \frac{\sum_{i=1}^{N}(\theta_i - \hat{\theta}_i)^2}{2\sigma_\theta^2} + \frac{\sum_{i=1}^{N}(\varphi_i - \hat{\varphi}_i)^2}{2\sigma_\varphi^2} \quad (51)$$

where

$$\hat{\theta}_i = \tan^{-1}\frac{\hat{x}-x_i}{\hat{y}-y_i},\ \hat{\varphi}_i = \tan^{-1}\frac{\hat{D}_i}{\hat{z}-z_i},\ \hat{D}_i = \sqrt{(\hat{x}-x_i)^2+(\hat{y}-y_i)^2}. \quad (52)$$

The hybrid ML function is

$$J = J_s + J_A. \quad (53)$$

To derive the CRLB, consider the Fisher Information Matrix [17]

$$\mathbf{FIM} = E\left\{\left[\frac{\partial J}{\partial \boldsymbol{\mu}}\right]\left[\frac{\partial J}{\partial \boldsymbol{\mu}}\right]^T\right\} \quad (54)$$

where

$$\boldsymbol{\mu} = [x \quad y \quad z \quad \eta_0]^T. \quad (55)$$

Then

$$\mathbf{CRLB} = \mathbf{FIM}^{-1} \quad (56)$$

and the RCRLB is

$$\mathrm{RCRLB} = \left[\mathrm{CRLB}_{11} + \mathrm{CRLB}_{22} + \mathrm{CRLB}_{33}\right]^{\frac{1}{2}}. \quad (57)$$

where CRLB_{ij} is the element in the i-th row and j-th column of the matrix CRLB.

REFERENCES

[1] D.J. Torrieri, *Principles of Military Communications Systems*, Artech House, Inc., 1981.

[2] Q. Kong, X. Yang and X. Xie, "A novel localization algorithm based on received signal strength ratio," *WiCOM*, 2008, pp. 1-6.

[3] X Li, "Collaborative localization with received-signal strength in wireless sensor networks," *IEEE Trans. on Vehicular Tech.*, 2007, pp.3807-3817.

[4] O. Ureten and T. J. Willink, "Joint estimation of emitter power and location in cognitive radio networks," *SPAWC*, 2011, pp. 61-65.

[5] S. Kim, H. Jean, H. Lee, and J. Ma, "Robust transmission power and position estimation in cognitive radar," in *Lecture Notes in Computer Science*, pp.719-728, Spinger Berlin/Heidleberg, 2008.

[6] H.C. So, "Source Localization: Algorithms and analysis," in *Handbook of Position Location: Theory, Practice, and Advances*, eds. S. Zekavat and M. Buehrer, Wiley-IEEE Press, 2011.

[7] Y.T. Chan and K. C. Ho, "A simple and efficient estimator for hyperbolic location," *IEEE Trans. on Signal Processing*, 1994, pp. 1905 –1915.

[8] K.B. Purvis, K.J. Astom and M. Khammash, "Estimation and optimal configuration for localization using cooperative UAVs," *IEEE Trans. on Control Systems Technology*, pp. 947-958, 2008

[9] K.B. Purvis, K.J. Astom and M. Khammash, "Estimating radar positions using cooperative unmanned air vehicle teams," *American Control Conf.*, pp. 3512-3517, 2005.

[10] E. Guerrero, J. Alvarez and L. Rivero, "3D-ADAL: A three-dimensional distributed range-free localization algorithm for wireless sensor networks based on unmanned aerial vehicles," *5th International Conf. on Digital Information Management (ICDIM)*, 2010.

[11] K. Dogancay, "UAV path planning for passive emitter localization," *IEEE Trans. on Aero. and Elect. Systems*, 2012, pp.1150-1166.

[12] S. Wang, B.R. Jackson and R. Inkol, "Hybrid RSS/AOA emitter location estimation based on least squares and maximum likelihood criteria," *CCECE*, 2012, pp.24-29.

[13] M. Laaraiedh, L. Yu, S. Avrillon and B. Uguen, "Comparison of hybrid localization schemes using RSSI, TOA, and TDOA," *Wireless European Conference*, 2011, pp.1-5.

[14] J. Chen and A. Abedi, "A hybrid framework for radio localization in broadband wireless systems," *Global Telecom. Conf.*, 2010, pp.1-6.

[15] S. Wang, R. Inkol and B.R. Jackson, "Relationship between the maximum likelihood emitter location estimators based on received signal strength (RSS) and received signal strength difference (RSSD)," *Queen's Biennial Symposium on Communications*, 2012, pp.64 - 69.

[16] Y.T. Chan, H.C. So, B.H. Lee, F. Chan, B. Jackson, and W. Read, "Angle-of-arrival localization of an emitter from air platforms," *CCECE*, 2013, pp. 1-5.

[17] H. Van Trees, *Detection, Estimation and Modulation Theory, Part I*,Wiley, New York, 2001.